

## Original Article

# Urine-derived stem cells as a model for age-related kidney degeneration and chronic disease risk

Pengfei Yu<sup>1,2\*</sup>, Jiaqi Li<sup>1\*</sup>, Huifen Ding<sup>2\*</sup>, Yu Chen<sup>1</sup>, Carol C Christina<sup>2</sup>, Anthony Bleyer<sup>3</sup>, Zhongping Duan<sup>1\*</sup>, Anthony Atala<sup>2</sup>, Yuanyuan Zhang<sup>2\*</sup>

<sup>1</sup>The Fourth Department of Liver Disease, Beijing Youan Hospital, Capital Medical University, Beijing 100069, China; <sup>2</sup>Wake Forest Institute for Regenerative Medicine, Wake Forest University Health Sciences, Winston-Salem, NC 27101, USA; <sup>3</sup>Department of Internal Medicine, Section on Gerontology and Geriatrics, Wake Forest University School of Medicine, Winston-Salem, NC 27157, USA. \*Equal contributors.

Received October 2, 2025; Accepted October 23, 2025; Epub October 25, 2025; Published October 30, 2025

**Abstract:** Renal aging contributes to declining kidney function and heightened susceptibility to chronic kidney disease (CKD). A key factor in this process is the diminished number and functionality of renal stem/progenitor cells, though the underlying mechanisms remain incompletely understood. Human urine-derived stem/progenitor cells (USCs) represent a promising, non-invasive source with notable regenerative potential. In this study, we examined cellular proliferation, reactive oxygen species (ROS) production, and senescence-associated protein expression as indicators of age-related degeneration in renal progenitor cells. USCs obtained from older healthy and diabetic individuals were compared to those from young, healthy donors. Our results demonstrate that USCs from aged and diabetic donors exhibit significantly reduced proliferation, elevated ROS levels, and increased  $\beta$ -galactosidase expression. Moreover, these cells showed impaired capacity to form 3D renal spheroids with tubular-like structures over a two-week culture period, relative to young controls. Together, these findings suggest that USCs from older or diabetic individuals - when cultured in both 2D and 3D systems - serve as a valuable model for studying renal aging and progenitor cell dysfunction. This model may facilitate the identification of biomarkers for renal aging and CKD risk and inform future regenerative and therapeutic strategies.

**Keywords:** Urine-derived stem cell, aging, diabetes

## Introduction

Kidney aging is a natural biological process marked by a progressive decline in renal function and structural integrity. It is a major risk factor for the development of age-related chronic kidney diseases (CKD), including diabetic nephropathy (DN) [1, 2]. A growing body of evidence suggests that the deterioration of renal stem/progenitor cells plays a critical role in this decline, yet the mechanisms underlying their degeneration remain poorly understood.

Human urine-derived stem cells (USCs), identified by our laboratory as renal progenitor cells (RPCs) [3-6], offer a promising and non-invasive cell source for studying kidney aging and regeneration. USCs are easily accessible, circumventing the need for invasive procedures, and possess robust self-renewal and differentiation

capacities. These properties have enabled their successful application in various precision medicine approaches [7-12].

Our recent findings revealed a compelling age-related decline in USC functionality: USCs isolated from older individuals (>65 years) exhibited significantly reduced stemness, differentiation potential, and regenerative capacity compared to those from younger donors (18-35 years) [13]. These observations suggest that USCs may serve not only as a therapeutic tool but also as a model system for investigating renal aging and health status.

In this study, we aim to further characterize age-related degeneration in USCs by examining reactive oxygen species (ROS) production, cellular senescence, proliferation, and 3D spheroid formation. We hypothesize that USCs de-

## Urine-derived stem cells in kidney aging

rived from older healthy or diabetic individuals exhibit signs of renal progenitor cell degeneration, including diminished proliferative capacity, elevated expression of the senescence marker  $\beta$ -galactosidase, and impaired ability to form renal-like spheroids. By comparing these cells to USCs from young, healthy donors, we seek to uncover key cellular defects associated with aging and diabetes.

Our findings may provide new insights into the mechanisms of renal progenitor cell dysfunction and offer a foundation for developing strategies to delay or reverse kidney aging through stem cell-based interventions.

### Materials and methods

#### *USC collection and cell culture*

Urine samples were collected from young, healthy donors aged 20-35 (n=6, Y-USC), older healthy adults aged 61-85 (n=6, O-USC), and elderly patients with DN aged 61-85 (n=6, D-USC). Diabetic nephropathy was defined as having chronic kidney function stage 2-3b, estimated glomerular filtration rate (eGFR) of 41-62, serum creatinine 1.25-1.65, and BUN of 23-52. The urine volume of each sample was recorded. USC was isolated from the urine samples by centrifugation and washed with 1X PBS. The cell pellet was resuspended in the modified culture medium described in the previous work [4], and the number of live cells and total cells in each sample were determined using trypan blue dye exclusion staining and counted with a hemocytometer. The remaining cell suspension was cultured in a 24-well plate (Thermo Fisher Science, Chicago, IL, USA). The medium was changed on the third day and every 2 days thereafter. The cell clones were continuously observed, and the date when the first and last clones appeared, as well as the total number of cell clones in each sample, were recorded. The standardized clone number was calculated by dividing the total clone number by the urine volume (ml) and then multiplying by 100 (ml).

#### *Morphology and proliferation of USCs*

All the cell clones were sub-cultured on day 21 and marked as passage 0 (p0). The cell morphology of each passage was continuously observed under a phase-contrast microscope (Leica, Germany) until passage 7. Pictures were

taken on the third day after sub-culturing, and the cell surface area was analyzed using Image J 1.53i (NIH, USA) (Java 1.8.0\_282). Cells were thresholded to remove the background to identify the whole-cell region of interest, and the cell surface area was measured.

The cell viability in the spheroids was determined using the Live/Dead assay (Thermo Fisher Science, Waltham, MA, USA). The USC spheroids were harvested and incubated in a working solution containing 2 mM Calcein AM and 4 mM EthD-1 in 1X PBS for 30 minutes at room temperature. The samples were rinsed with 1X PBS twice and observed using a confocal microscope (Leica TCS-LSI, Leica Biosystems Inc., Buffalo Grove, IL, USA). Photos were taken, and the intensity of red fluorescence (indicating dead cells) and green fluorescence (indicating live cells) were measured using ImageJ software. The viability of the cells in spheroids was analyzed accordingly.

#### *USC doubling time*

The USC doubling time (DT) analysis was conducted by seeding 1,000 cells into each well of 96-well plates (Thermo Fisher Science), followed by the cell count kit-8 (CCK-8, Dojindo, Japan) assay. Briefly, the medium was replaced with fresh medium containing 10% CCK-8 reagent at 4 and 24 hours. After incubation at 37°C for 2 hours, the medium from each well was carefully transferred to a new 96-well plate to read the absorbance at 450 nm using a plate reader (MultiSkan FC, Thermo, USA). The cell numbers at 4 hours and 24 hours were calculated according to the CCK-8 assay. The DT was calculated using the following formula:

$DT = 24 \times [\lg 2 / (\lg N_t - \lg N_0)]$  [12].  $N_0$  is the original number of seeded cells, which was tested at 4 hours after seeding.  $N_t$  is the cell number tested after being cultured for 24 hours.

#### *Generation of silk fiber matrix*

Silk fibroin was extracted from silk cocoons (TTSAM, China) employing established methodologies as previously reported [14]. A 10% silk fibroin electrospinning solution and a random-structured matrix were prepared through a wet process. To fabricate sponge-like silk fiber matrices (SFM), the matrices underwent immersion in 100% ethanol (Warner Graham

## Urine-derived stem cells in kidney aging

Company, USA) for a duration of up to 45 minutes, followed by complete cross-linking and subsequent washing. Following this treatment, SFM samples were frozen with deionized water in 6 cm diameter culture dishes (Corning, NY) and subsequently subjected to a 3-day lyophilization process. The resulting SFM specimens were meticulously crafted utilizing 4 mm diameter and 0.2 mm thickness Biopsy Dermal Punches (Painful Pleasures, USA).

### *Senescence-associated SA- $\beta$ -Gal activity assay*

Part of the cells were seeded on a 6-well plate during subculturing. SA- $\beta$ -Gal activity was detected using the Senescence Detection Kit (Abcam) after 3 days. Cells were rinsed with 1 $\times$  PBS and fixed in a 4% paraformaldehyde solution for 10 minutes at room temperature. After rinsing again, a staining solution mix (470  $\mu$ l staining solution, 5  $\mu$ l staining supplement, and 25  $\mu$ l 20 mg/ml X-gal in DMF) was added to each well and incubated at 37°C overnight. The cells were observed using the Olympus IX-70 fluorescence microscope. Pictures were taken under multiple fields per well from three samples per group. The total number of cells was counted, and the cells with blue staining (SA- $\beta$ -gal) were counted as senescence-positive cells. The percentage of senescence-positive cells was calculated, and individual values were plotted using GraphPad Prism. Statistical significance was calculated by the Holm-Šidák method for multiple unpaired t-tests, with a *P*-value of <0.05 considered a significant difference.

### *3D spheroid formation*

USC at passage 4 (p4) were seeded in low-attached ULA 96-well plates (Corning, Glendale, AZ, USA) to form 3D spheroids. The USC 3D spheroids were observed by phase-contrast microscopy on day 3, week 2, and week 4. Well-organized spheroids were observed for most of the samples on day 3, while cells from some samples failed to form 3D spheroids even after being cultured for 2 weeks. The medium was changed every 3 days, and the ratio of spheroid formation was calculated by dividing the number of samples that formed spheroids by the total number of samples.

### *H&E staining*

Two and four weeks after culture, the USC spheroids were harvested and fixed in a 4%

paraformaldehyde solution for 30 minutes at room temperature. They were then rinsed with 1X PBS, equally embedded in HistoGel (Thermo Fisher), and immersed in 70% EtOH for 2 days. The dehydrated HistoGel blocks were embedded in paraffin and cut into 6  $\mu$ m thick sections. H&E staining of the sections was performed using a Leica Histochemical Autostainer.

### *ROS assay*

USC at p4 were seeded in a dark, clear-bottom 96-well microplate with 25,000 cells per well, allowing overnight adherence. The media was replaced with 100  $\mu$ L/well of 1X Buffer, the buffer was then removed, and the cells were stained by adding 100  $\mu$ L/well of the diluted DCFDA Solution. The cells were incubated with the diluted DCFDA Solution for 45 minutes at 37°C in the dark. After the incubation, the DCFDA Solution was removed and replaced with 100  $\mu$ L/well of 1X Buffer, 1X Supplemented Buffer (2 mL FBS to 18 mL of 1X Buffer). Finally, the plate was measured immediately on a fluorescence plate reader at Ex/Em =485/535 nm in endpoint mode.

### *Statistical analysis*

Descriptive statistics are presented as mean  $\pm$  standard deviation (SD) using OriginLab software version Pro2025. All data were derived from experiments independently repeated at least three times. For experiments with multiple treatments, such as varying doses, one-way ANOVA with Dunnett's multiple comparisons to the control group (DMSO) or multiple unpaired t-tests were employed. For experiments with two groups, such as different time points, Student's t-test was used for comparisons, with Bonferroni's multiple comparisons applied when appropriate. A *p*-value of <0.05 was considered statistically significant.

## **Results**

### *USC culture and age-related dynamics*

Cell clones were consistently identified in all examined urine samples. The quantitative metrics, encompassing total cell count, viable cell count, and overall clone count, showed no discernible correlation with donor age or the presence of diabetic nephropathy (DN) although initial cell clones of Y-USC appeared earlier than those of O-USC and D-USC. In addition,

## Urine-derived stem cells in kidney aging

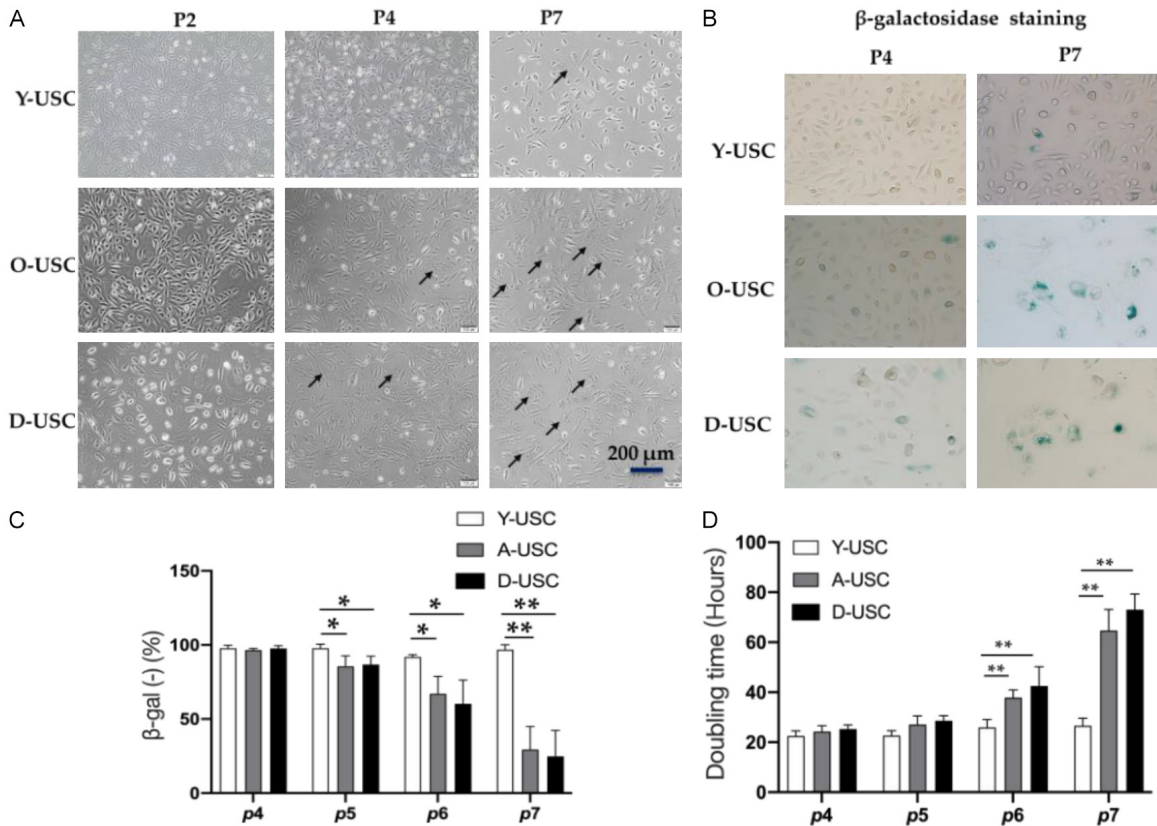


**Figure 1.** Alterations in cell morphology and proliferation of USC with passages. (A) Cell morphology changes of O-USC and D-USC, compared to Y-USC under phase-contrast microscopy. Arrows indicate senescent cells with enlarged and flattened morphology. (B) Change in the number of O-USC and D-USC expressing  $\beta$ -galactosidase with passages, compared to Y-USC cells on 2D culture, assessed by immunocytochemical staining; (C) Semi-quantitative analysis for (B). (D) Changes in cell doubling time of O-USC and D-USC compared to Y-USC, assessed using the CCK-8 method. USCs from 3 groups were at p4. Results are the Mean  $\pm$  SEM, n=5-6 per group. \*P<0.05, \*\*P<0.01.

these parameters were determined to be unrelated to urine volume. Noteworthy is the observation that clones originating from USC in young, healthy donors exhibited an earlier expansion compared to those in donors from the other two groups (Table 1). This finding suggests a potential age-related influence on the temporal emergence of USC clones in urinary specimens.

In primary cell clone identification, USC clones were consistently identified in all examined urine samples. Quantitative analysis revealed no significant correlation between total cell count, viable cell count, overall clone count, donor age, presence of diabetic nephropathy (DN), or urine volume. Interestingly, initial cell clones of Y-USC appeared earlier than those of older USC (O-USC) and diabetic USC (D-USC) (Table 1). This suggests a potential influence of age on the temporal emergence of USC clones in urinary specimens.

### Cellular senescence

In initial passages, O-USC and D-USC initially exhibited a “rice grain” morphology, similar to USC. All cell lineages successfully grew until passage 7 (p7). By p7, approximately 25% of O-USC and D-USC displayed increased cell size and vacuoles, while Y-USC remained unchanged (Figure 1A). Senescent cells typically exhibit enlarged size and positive staining for senescence-associated beta-galactosidase (SA- $\beta$ -Gal) activity. At passage 4, cell size and SA- $\beta$ -Gal staining were comparable across all groups. With increasing passages, O-USC and D-USC displayed a significant rise in cell size and senescent cells compared to Y-USC (Figure 1B, 1C). Particularly, the incidence of senescent cells was significantly higher in O-USC and D-USC beyond passage 4 (Figure 1C). These findings suggest that age and diabetes influence cellular senescence dynamics.

## Urine-derived stem cells in kidney aging

**Table 1.** USC data generated from older adults, DN patents, compared to younger adults

	Urine volume (ml)	No. of live cells/ Total no. of cells	Ratio of live cells	First cell clones appearance (days)	Total number of clones	Standardized Clone number./100 ml	Spheroid Formation on day 3	Numbers of tubule formation per spheroid	USC attached on silk fibers
<b>Y-USC</b>									
#1	127	1.5*10 <sup>4</sup> /4.8*10 <sup>4</sup>	31.3%	4	10	7.9	yes	3	MLs
#2	100	4.4*10 <sup>3</sup> /4.6*10 <sup>4</sup>	9.6%	6	26	26	yes	6	MLs
#3	200	1.0*10 <sup>5</sup> /2.4*10 <sup>5</sup>	41.7%	2	26	13	yes	11	MLs
#4	50	8*10 <sup>4</sup> /5.4*10 <sup>5</sup>	14.8%	2	5	10	yes	0	MLs
#5	200	7*10 <sup>4</sup> /1*10 <sup>5</sup>	70.0%	4	10	5	yes	0	MLs
#6	270	1*10 <sup>4</sup> /9*10 <sup>4</sup>	11.1%	4	2	0.7	yes	4	MLs
	In Sum: (Mean ± SEM)		29.7%±3.9%	3.7±0.3	13.2±1.7	10.4±1.5		4.0±0.7	
<b>O-USC</b>									
#1	82	2*10 <sup>4</sup> /22.5*10 <sup>4</sup>	8.9%	6	10	12.2	yes	3	MLs
#2	200	2*10 <sup>4</sup> /4*10 <sup>4</sup>	50.0%	12	1	0.5	no	NA	No
#3	207	3*10 <sup>4</sup> /5.5*10 <sup>4</sup>	54.5%	6	20	9.7	yes	4	MLs
#4	177	1.5*10 <sup>4</sup> /6*10 <sup>4</sup>	25.0%	6	21	11.9	yes	0	ML
#5	200	5*10 <sup>2</sup> /3*10 <sup>3</sup>	16.7%	5	6	3	yes	4	ML
#6	290	0.3*10 <sup>4</sup> /1.8*10 <sup>4</sup>	16.7%	6	6	2.1	yes	13	No
	In Sum: (Mean ± SEM)		28.6%±3.2%	6.8±0.4	10.7±1.4	6.6±0.9		4.8±1.0	
<b>D-USC</b>									
#1	30	3.5*10 <sup>4</sup> /7*10 <sup>4</sup>	50.0%	5	7	23, 3	yes	2	ML
#2	200	0.6*10 <sup>4</sup> /0.8*10 <sup>5</sup>	7.5%	8	1	0.5	no	NA	No
#3	240	6.5*10 <sup>4</sup> /9*10 <sup>4</sup>	72.2%	4	4	1.7	yes	3	No
#4	150	10*10 <sup>4</sup> /5*10 <sup>4</sup>	20.0%	6	3	2	yes	0	ML
#5	80	0.25*10 <sup>4</sup> /3*10 <sup>4</sup>	8.3%	6	14	17.5	yes	8	ML
#6	58	1.5*10 <sup>4</sup> /8.5*10 <sup>4</sup>	17.6%	8	6	10.3	yes	5	No
	In Sum: (Mean ± SEM)		29.3%±4.4%	6.2±0.3	5.8±0.8	6.4±1.2		3.6±0.6	

Notes: MLs: Multiple-layers; ML: Mono-layer.

**Table 2.** Protein levels of reactive oxygen species in three groups of USC spheroids assessed by ELISA

	Pt 1	Pt 2	Pt 3	Pt 4	Pt 5	Pt 6	Mean ± SEM
Y-USC	0.512	0.5447	0.552	0.534	0.481	0.546	0.53±0.005
O-USC	0.584	0.623	0.582	0.624	0.583	0.512	0.59±0.007
D-USC	0.564	0.616	0.638	0.623	0.572	0.658	0.61±0.004

Note: Pt-patient; Y-USC, O-USC, and D-USC: USC were obtained from healthy young, old individuals, and older diabetic patients.

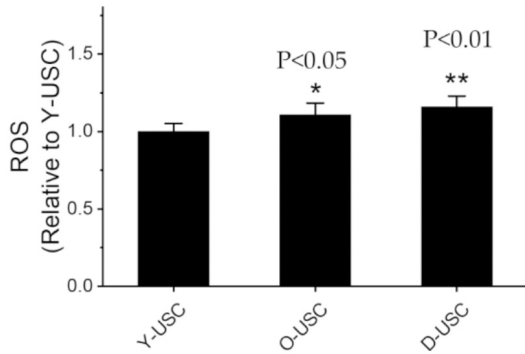


**Figure 2.** Protein levels of reactive oxygen species (ROS) in O-USC and D-USC compared to Y-USC. Changes in the protein levels of reactive oxygen species (ROS) were assessed by ELISA in urinary stem cells (USCs) from three groups (O-USC, D-USC, and Y-USC) at passage 4 (p4). Results are presented as the Mean ± SEM, with n=5-6 per group. Statistical significance is denoted by \*P<0.05 and \*\*P<0.01.

In the cell proliferation assessment, the doubling time of O-USC and D-USC significantly increased, particularly after p5, while Y-USC maintained a steady doubling time (Figure 1D). This negatively affect the vitality in O-USC and D-USC compared to Y-USC. Y-USC cells maintain a consistent growth rate, whereas O-USC and D-USC experience a progressive decline in growth dynamics across passages. Overall, these findings suggest that age and diabetes contribute to cellular senescence and decreased proliferation in O-USC and D-USC compared to Y-USC.

#### Reactive oxygen species

To assess the potential for age-related oxidative stress, protein levels of O-USC and D-USC were evaluated in comparison to Y-USC using ELISA (Table 2). Figure 2 reveals a statistically significant increase in ROS levels for both O-USC and D-USC compared to Y-USC. However, no significant difference in ROS levels was observed between O-USC and D-USC.

#### Morphology and viability of USC spheroids

The size of all USC spheroids from the three groups remained the same for 4 weeks but decreased after 5 weeks of culture. Notably, in the O-USC and D-USC groups, a larger proportion of cells on the spheroid surfaces exhibited increased size and began to detach from the spheroid after week 4. In addition, central necrosis manifested earlier in the O-USC and D-USC groups, with one in six samples from both the O-USC and D-USC groups failing to form spheroids. The cells were completely separated from each other or easily torn apart when medium was added or washed for testing. In contrast, the fewer dead cells and higher viability in the center of spheroids of Y-USC and all spheroids remained well over 4 weeks (Figures 3 and 4; Table 1). In this 3D USC spheroids model, distinct renal tubular-like structures were more prevalent in the D-USC group compared to the Y-USC and O-USC groups, as evidenced by H&E staining of the 3D spheroids.

#### 3D culture of USC seeded on SFM

To evaluate the effect of age of USC on cell adhesion to matrix scaffold, USC from three groups were seeded on 3D culture of SFM for 3 days. Most Y-USC showed the ability to attach to the silk fiber matrix and form multiple layers (3-4 layers of cells on a single silk fiber) in 3D SFM, while O-USC formed only one or two layers on silk fiber in 4/6 samples and in half of the D-USC samples, with most forming a monolayer on the silk fiber (Figure 3; Table 1).

#### Discussion

Renal progenitor cells (RPCs) are essential for kidney repair and regeneration [11]. However, their function declines with age and in diabetes [15], contributing to increased susceptibility to chronic kidney disease (CKD). This study investigated the degeneration of RPCs in aging and diabetic conditions using human urine-derived

## Urine-derived stem cells in kidney aging

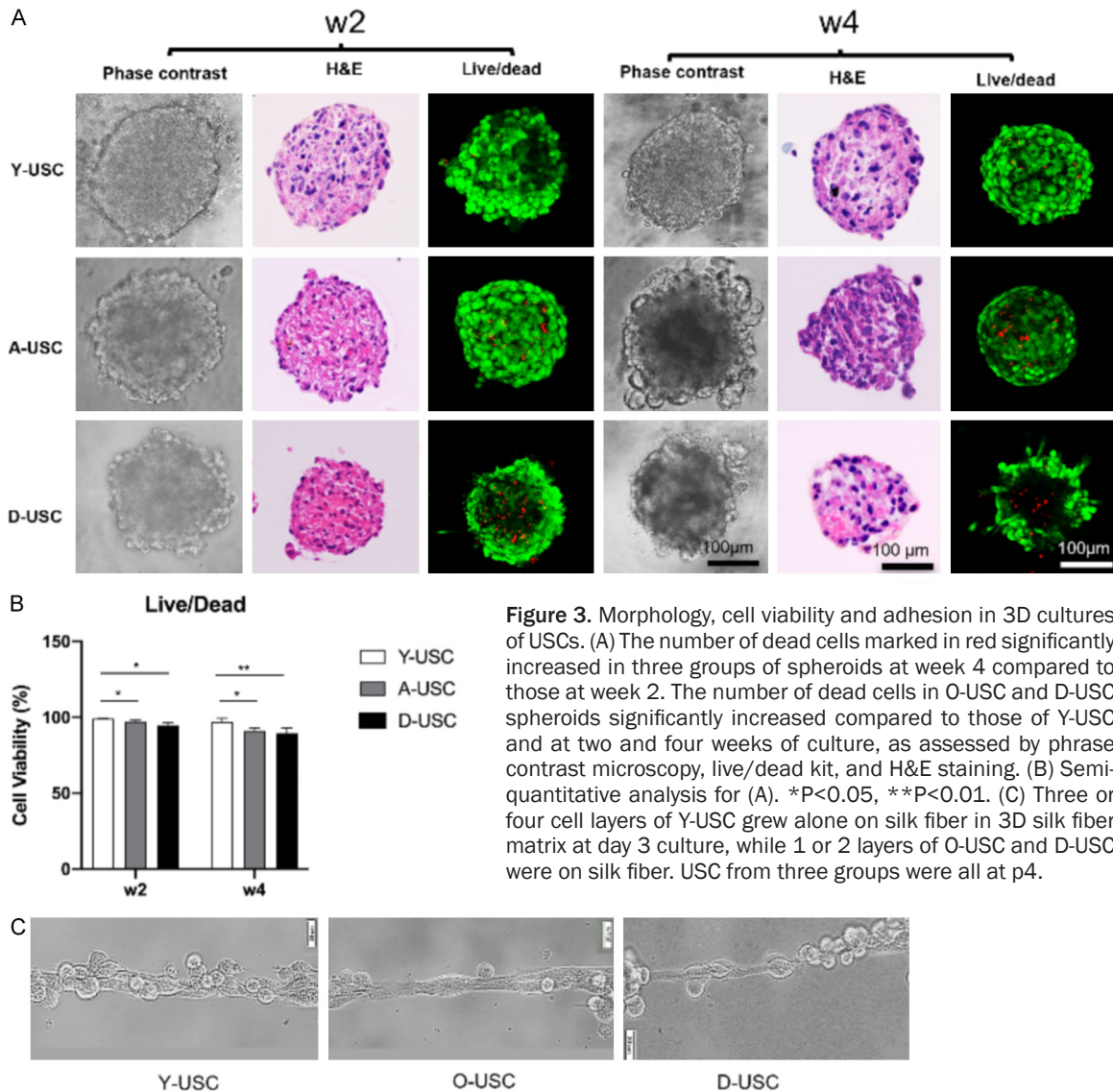


**Figure 3.** Morphology, cell viability and adhesion in 3D cultures of USCs. (A) The number of dead cells marked in red significantly increased in three groups of spheroids at week 4 compared to those at week 2. The number of dead cells in O-USC and D-USC spheroids significantly increased compared to those of Y-USC and at two and four weeks of culture, as assessed by phase contrast microscopy, live/dead kit, and H&E staining. (B) Semi-quantitative analysis for (A). \* $P < 0.05$ , \*\* $P < 0.01$ . (C) Three or four cell layers of Y-USC grew alone on silk fiber in 3D silk fiber matrix at day 3 culture, while 1 or 2 layers of O-USC and D-USC were on silk fiber. USC from three groups were all at p4.

stem cells (USCs) as a model. Our findings demonstrate that USCs from older adults without diabetes (O-USCs) and those with diabetic nephropathy (D-USCs) exhibit significantly impaired regenerative capacity compared to USCs from young healthy individuals. This dysfunction was associated with delayed clonal emergence, reduced proliferation, elevated reactive oxygen species (ROS) production, increased expression of senescence markers, and diminished ability to form 3D renal spheroids.

These results suggest that mitochondrial dysfunction may be a central driver of RPC senescence and impaired function, potentially explaining the increased vulnerability to kidney disease in aging and diabetes. Mitochondrial

impairment not only reduces energy production but also generates excessive ROS, which damage cellular components and promote senescence and apoptosis [16].

Kidney aging is characterized by a decline in glomerular filtration rate (GFR), reflecting reduced capacity to filter blood and maintain homeostasis [17, 18]. This decline is accompanied by histological changes, including nephron loss, reduced renal perfusion, arterial stiffening, thickening of the glomerular basement membrane, and increased interstitial fibrosis [19-23]. Our findings suggest that the metabolic and regenerative defects observed in O-USCs and D-USCs may contribute to these pathological features.

## Urine-derived stem cells in kidney aging

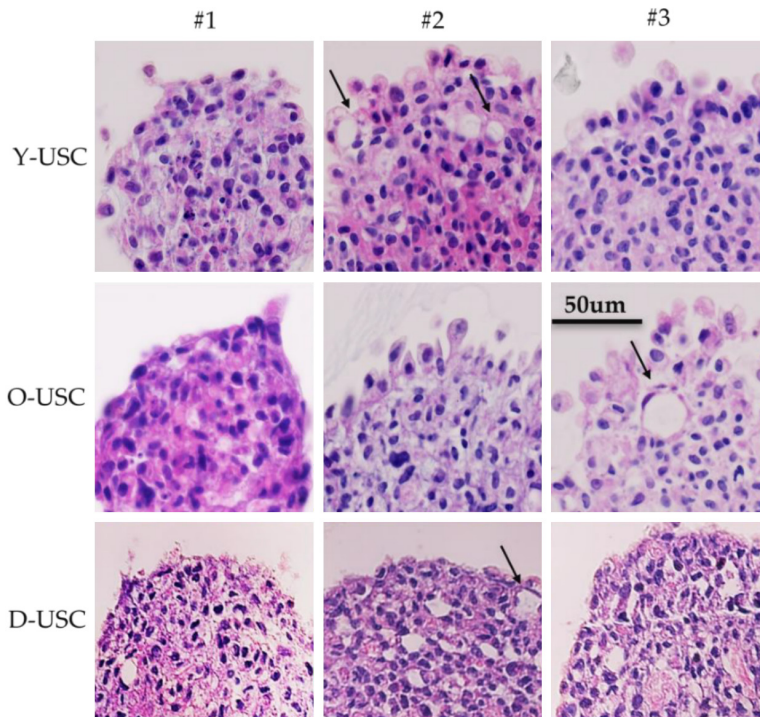


**Figure 4.** Formation of renal tubular-like structures in 3D renal spheroids. This figure shows renal tubular-like structures observed on the surface zone of 3D renal spheroids after two weeks of culture. Spheroids derived from Y-USC (n=3 at P4) are compared with those from O-USC (n=3) and D-USC (n=3). Sections were stained with Hematoxylin and Eosin (H&E).

Degeneration of RPCs has profound implications for kidney aging. Loss of regenerative function impairs the kidney's ability to repair damage, accelerating the progression of CKD [24]. This study highlights the metabolic heterogeneity of USCs across age and disease states, offering a valuable model for dissecting the molecular mechanisms underlying renal aging and diabetic nephropathy. Future research should focus on identifying key molecular drivers of these metabolic changes, such as mitochondrial regulators, oxidative stress pathways, and epigenetic modifications. Additionally, correlating USC metabolic profiles with clinical outcomes in elderly and diabetic patients could yield predictive biomarkers and therapeutic targets.

Cellular senescence, defined as a state of irreversible growth arrest, is a hallmark of aging tissues [25, 26]. Senescent cells accumulate in the kidney with age and contribute to functional decline [27]. Senescence-associated  $\beta$ -galactosidase (SA- $\beta$ -gal) is a widely used marker for identifying senescent cells [28-30]. In our study, SA- $\beta$ -gal-positive USCs were significantly

more abundant in older and diabetic donors, indicating that aging and diabetes promote senescence in renal progenitor populations. Targeting senescence pathways may offer new therapeutic strategies to preserve kidney function in these populations.

Our data reinforce the role of mitochondrial dysfunction in age-related renal decline. Elevated ROS levels in O-USCs and D-USCs were accompanied by reduced proliferation and increased senescence, consistent with a state of chronic oxidative stress. These findings support the hypothesis that mitochondrial damage is a key contributor to progenitor cell exhaustion and impaired regeneration.

By examining USC clonal dynamics, we gained insights into the aging process at the cellular level. Clonal expansion was delayed in aged and diabetic donors, suggesting slower or less efficient self-renewal. In addition, cell growth rates declined with passage, and cell size increased - hallmarks of senescence. These changes reflect altered cellular dynamics and reduced regenerative potential.

The ability to form 3D spheroids - miniature organoids that mimic renal architecture - was significantly compromised in O-USCs and D-USCs. These spheroids exhibited fewer tubular structures and weaker adhesion to silk scaffolds, indicating impaired differentiation and interaction with the extracellular matrix. Reduced integrin expression, potentially driven by DNA damage, epigenetic alterations, oxidative stress, and inflammation [31], may underlie these adhesion defects.

Together, these findings paint a comprehensive picture of how aging and diabetes impair renal progenitor cell function. Delayed clonal expansion, reduced proliferation, increased senescence, impaired spheroid formation, and weakened adhesion all point to a decline in regen-

erative capacity. Understanding the molecular basis of these changes - particularly the roles of mitochondrial dysfunction and integrin signaling - could inform the development of interventions to preserve RPC function and slow kidney aging [32-34].

In conclusion, this study provides compelling evidence that mitochondrial dysfunction is a key driver of RPC degeneration in aging and diabetes. USCs from older and diabetic individuals exhibit reduced proliferation, elevated ROS levels, increased senescence, and impaired 3D spheroid formation. These cells are highly sensitive to age- and diabetes-induced metabolic stress, making them a promising model for identifying biomarkers and predicting renal function decline. Our findings lay the groundwork for future therapeutic strategies aimed at restoring progenitor cell function and mitigating kidney aging.

### Acknowledgements

We acknowledge the support from the National Institutes of Health through the National Institute of Allergy and Infectious Diseases (R21AI152832, R03AI165170) and the National Eye Institute (R21EY035833); the U.S. Department of Defense under the Idea Development Award HT94252510856 (to Y.Z.); and the Beijing YouAn Hospital, Capital Medical University Young and Mid-Career Investigator Incubation Program BJYAYY-YN2024-17 (to P.Y.).

### Disclosure of conflict of interest

None.

**Address correspondence to:** Dr. Yuanyuan Zhang, Wake Forest Institute for Regenerative Medicine, Wake Forest University School of Medicine, Medical Center Boulevard, Winston-Salem, NC 27157, USA. E-mail: Yuanyuan.Zhang@advocatehealth.org; Dr. Zhongping Duan, The Fourth Department of Liver Disease, Beijing Youan Hospital, Capital Medical University, Beijing 100069, China. E-mail: duan@ccmu.edu.cn

### References

[1] Kanasaki K, Kitada M and Koya D. Pathophysiology of the aging kidney and therapeutic interventions. *Hypertens Res* 2012; 35: 1121-1128.

[2] Fang Y, Gong AY, Haller ST, Dworkin LD, Liu Z and Gong R. The ageing kidney: molecular mechanisms and clinical implications. *Ageing Res Rev* 2020; 63: 101151.

[3] Bharadwaj S, Liu G, Shi Y, Wu R, Yang B, He T, Fan Y, Lu X, Zhou X, Liu H, Atala A, Rohozinski J and Zhang Y. Multipotential differentiation of human urine-derived stem cells: potential for therapeutic applications in urology. *Stem Cells* 2013; 31: 1840-1856.

[4] Zhang Y, McNeill E, Tian H, Soker S, Andersson KE, Yoo JJ and Atala A. Urine derived cells are a potential source for urological tissue reconstruction. *J Urol* 2008; 180: 2226-2233.

[5] Bharadwaj S, Liu G, Shi Y, Markert C, Andersson KE, Atala A and Zhang Y. Characterization of urine-derived stem cells obtained from upper urinary tract for use in cell-based urological tissue engineering. *Tissue Eng Part A* 2011; 17: 2123-2132.

[6] Huang RL, Li Q, Ma JX, Atala A and Zhang Y. Body fluid-derived stem cells - an untapped stem cell source in genitourinary regeneration. *Nat Rev Urol* 2023; 20: 739-761.

[7] Guo H, Deng N, Dou L, Ding H, Criswell T, Atala A, Furdui CM and Zhang Y. 3-D human renal tubular organoids generated from urine-derived stem cells for nephrotoxicity screening. *ACS Biomater Sci Eng* 2020; 6: 6701-6709.

[8] Yang Q, Chen W, Han D, Zhang C, Xie Y, Sun X, Liu G and Deng C. Intratunical injection of human urine-derived stem cells derived exosomes prevents fibrosis and improves erectile function in a rat model of Peyronie's disease. *Andrologia* 2020; 52: e13831.

[9] Liu G, Wu R, Yang B, Shi Y, Deng C, Atala A, Mou S, Criswell T and Zhang Y. A cocktail of growth factors released from a heparin hyaluronic-acid hydrogel promotes the myogenic potential of human urine-derived stem cells in vivo. *Acta Biomater* 2020; 107: 50-64.

[10] Xiong G, Tao L, Ma WJ, Gong MJ, Zhao L, Shen LJ, Long CL, Zhang DY, Zhang YY and Wei GH. Urine-derived stem cells for the therapy of diabetic nephropathy mouse model. *Eur Rev Med Pharmacol Sci* 2020; 24: 1316-1324.

[11] Zhang C, George SK, Wu R, Thakker PU, Abolbashari M, Kim TH, Ko IK, Zhang Y, Sun Y, Jackson J, Lee SJ, Yoo JJ and Atala A. Reno-protection of urine-derived stem cells in a chronic kidney disease rat model induced by renal ischemia and nephrotoxicity. *Int J Biol Sci* 2020; 16: 435-446.

[12] Ling X, Zhang G, Xia Y, Zhu Q, Zhang J, Li Q, Niu X, Hu G, Yang Y, Wang Y and Deng Z. Exosomes from human urine-derived stem cells enhanced neurogenesis via miR-26a/HDAC6 axis after ischaemic stroke. *J Cell Mol Med* 2020; 24: 640-654.

## Urine-derived stem cells in kidney aging

- [13] Shi Y, Liu G, Wu R, Mack DL, Sun XS, Maxwell J, Guan X, Atala A and Zhang Y. Differentiation capacity of human urine-derived stem cells to retain telomerase activity. *Front Cell Dev Biol* 2022; 10: 890574.
- [14] Ding H, Zhong J, Xu F, Song F, Yin M, Wu Y, Hu Q and Wang J. Establishment of 3D culture and induction of osteogenic differentiation of pre-osteoblasts using wet-collected aligned scaffolds. *Mater Sci Eng C Mater Biol Appl* 2017; 71: 222-230.
- [15] Xiong G, Tang W, Zhang D, He D, Wei G, Atala A, Liang XJ, Bleyer AJ, Bleyer ME, Yu J, Aloji JA, Ma JX, Furdui CM and Zhang Y. Impaired regeneration potential in urinary stem cells diagnosed from the patients with diabetic nephropathy. *Theranostics* 2019; 9: 4221-4232.
- [16] Davalli P, Mitic T, Caporali A, Lauriola A and D'Arca D. ROS, cell senescence, and novel molecular mechanisms in aging and age-related diseases. *Oxid Med Cell Longev* 2016; 2016: 3565127.
- [17] Noronha IL, Santa-Catharina GP, Andrade L, Coelho VA, Jacob-Filho W and Elias RM. Glomerular filtration in the aging population. *Front Med (Lausanne)* 2022; 9: 769329.
- [18] Glasscock RJ and Rule AD. The implications of anatomical and functional changes of the aging kidney: with an emphasis on the glomeruli. *Kidney Int* 2012; 82: 270-277.
- [19] Dybiec J, Szlagor M, Młynarska E, Rysz J and Franczyk B. Structural and functional changes in aging kidneys. *Int J Mol Sci* 2022; 23: 15435.
- [20] Weinstein JR and Anderson S. The aging kidney: physiological changes. *Adv Chronic Kidney Dis* 2010; 17: 302-307.
- [21] Hommos MS, Glasscock RJ and Rule AD. Structural and functional changes in human kidneys with healthy aging. *J Am Soc Nephrol* 2017; 28: 2838-2844.
- [22] Rule AD, Amer H, Cornell LD, Taler SJ, Cosio FG, Kremers WK, Textor SC and Stegall MD. The association between age and nephrosclerosis on renal biopsy among healthy adults. *Ann Intern Med* 2010; 152: 561-567.
- [23] Gewin LS. Renal fibrosis: primacy of the proximal tubule. *Matrix Biol* 2018; 68-69: 248-262.
- [24] Bhatia D, Capili A and Choi ME. Mitochondrial dysfunction in kidney injury, inflammation, and disease: potential therapeutic approaches. *Kidney Res Clin Pract* 2020; 39: 244-258.
- [25] Kumari R and Jat P. Mechanisms of cellular senescence: cell cycle arrest and senescence associated secretory phenotype. *Front Cell Dev Biol* 2021; 9: 645593.
- [26] Campisi J and d'Adda di Fagagna F. Cellular senescence: when bad things happen to good cells. *Nat Rev Mol Cell Biol* 2007; 8: 729-740.
- [27] Sturmlechner I, Durik M, Sieben CJ, Baker DJ and van Deursen JM. Cellular senescence in renal ageing and disease. *Nat Rev Nephrol* 2017; 13: 77-89.
- [28] Valieva Y, Ivanova E, Fayzullin A, Kurkov A and Igrunkova A. Senescence-associated  $\beta$ -galactosidase detection in pathology. *Diagnostics (Basel)* 2022; 12: 2309.
- [29] Dimri GP, Lee X, Basile G, Acosta M, Scott G, Roskelley C, Medrano EE, Linskens M, Rubelj I, Pereira-Smith O, et al. A biomarker that identifies senescent human cells in culture and in aging skin in vivo. *Proc Natl Acad Sci U S A* 1995; 92: 9363-9367.
- [30] Kurz DJ, Decary S, Hong Y and Erusalimsky JD. Senescence-associated (beta)-galactosidase reflects an increase in lysosomal mass during replicative ageing of human endothelial cells. *J Cell Sci* 2000; 113: 3613-3622.
- [31] Borghesan M and O'Loughlen A. Integrins in senescence and aging. *Cell Cycle* 2017; 16: 909-910.
- [32] Forbes JM and Cooper ME. Mechanisms of diabetic complications. *Physiol Rev* 2013; 93: 137-188.
- [33] Ratliff BB, Abdulmahdi W, Pawar R and Wolin MS. Oxidant mechanisms in renal injury and disease. *Antioxid Redox Signal* 2016; 25: 119-146.
- [34] Bhargava P and Schnellmann RG. Mitochondrial energetics in the kidney. *Nat Rev Nephrol* 2017; 13: 629-646.